International Journal of Pharmaceutics 570 (2019) 118516

Contents lists available at ScienceDirect

International Journal of Pharmaceutics

journal homepage: www.elsevier.com/locate/ijpharm

Polyoxazolines based mixed micelles as PEG free formulations for an effective quercetin antioxidant topical delivery

L. Simon, M. Vincent, S. Le Saux, V. Lapinte, N. Marcotte, M. Morille, C. Dorandeu, J.M. Devoisselle, S. Bégu*

ICGM, Montpellier University, CNRS, ENSCM, Montpellier, France

ARTICLE INFO

Keywords:
Topical delivery
Antioxidant
Hybrid vesicle
Polyoxazolines
PEG free
Skin protection

ABSTRACT

This study aims to prove the value of the polyoxazolines polymer family as surfactant in formulations for topical application and as an alternative to PEG overuse. The amphiphilic polyoxazolines (POx) were demonstrated to have less impact on cell viability of mice fibroblasts (NIH3T3) than their PEG counterparts. Mixed micelles, made of POx and phosphatidylcholine, were manufactured using thin film and high pressure homogenizer process. The mixed micelles were optimized to produce nanosized vesicles of about 20 nm with a spherical shape and stable over 28 days. The natural lipophilic antioxidant, quercetin, was successfully encapsulated (encapsulation efficiency 94 ± 4% and drug loading 3.6 ± 0.2%) in the mixed micelles with no morphological variation. Once loaded in the formulation, the quercetin impact on cell viability of NIH3T3 was decreased while its antioxidant activity remained unchanged. This work highlights the capacity of amphiphilic POx to create, in association with phospholipids, stable nanoformulations which show promise for topical delivery of antioxidant and ensure skin protection against oxidative stress.

1. Introduction

With a surface of 2 m^2, the skin is the most extended organ of the human body acting as barrier to mechanical and chemical aggressions (Marks and Miller, 2019). It plays a key role in protecting the body from daily toxic aggressions due to environmental pollutants by generating reactive oxygen species (ROS) (Valacchi et al., 2012). This overproduction of ROS unbalances the antioxidant defense system of the human body (Poljšak et al., 2011) leading to oxidative stress that can create skin damage like premature skin aging (Rinnerthaler et al., 2015) but also skin cancer risks (Baudouin et al., 2002). Among the environmental sources responsible for skin damage (Krutmann et al., 2017), UV radiations were unambiguously shown to cause skin cancers (Valacchi et al., 2012). UVAs were more especially identified to induce DNA mutations *in fine* generating skin carcinogenesis. Other environmental pollutants, such as polycyclic aromatic hydrocarbons, cigarette smoke constituents and ozone, are also considered today as accountable for skin pathologies and cutaneous cancers (Baudouin et al., 2002).

To avoid the deleterious excess of ROS, antioxidant can be administrated through the skin. This topical delivery strategy uses natural or synthetic exogeneous molecules, with low or high molecular weight, as antioxidants (Andreia et al., 2011). Among all the natural compounds to be delivered, the highly lipophilic polyphenolic molecules belonging to the flavonoids family are often preferred for their powerful antioxidant properties and multiple pathways of activities (Nagula and Wairkar, 2019). Quercetin is one of the flavonols of interest for topical delivery since it gathers the properties of antioxidant and anti-inflammatory activities, wound healing and skin aging retardation. However, its low water solubility, instability to light and poor skin permeability (Hatahet et al., 2016a) require its formulation for an efficient activity. Therefore, various formulations such as smart crystals (Hatahet et al., 2016b), lipid nanocapsules (Hatahet et al., 2017), liposomes (Hatahet et al., 2018), solid lipid nanosystems (Bose et al., 2013), vesicles (Chessa et al., 2011), nanostructured lipid carriers (Chen-yu et al., 2012), nanoparticles (Tan et al., 2011), microemulsions (Martena et al., 2012) and lipid-based nanosystems (Caddeo et al., 2014) have been developed to enhanced the topical delivery of quercetin. It should be noted that most of these formulations use poly (ethylene glycol) (PEG) as stabilizer or thickener because of its very interesting properties including biocompatibility, low toxicity, high solubility in aqueous media and stealth behavior. This explains the PEG overuse for cosmetic and pharmaceutical applications (Shen et al., 2018) and its success as the “gold standard” for drug delivery. Recently, clinical awareness on PEG overuse for oral and parenteral delivery pointed out safety issues associated with an increase of PEG antibodies (Lubich et al., 2016) and the possible accumulation of the polymer in

* Corresponding author.

https://doi.org/10.1016/j.ijpharm.2019.118516
Received 26 April 2019; Received in revised form 9 July 2019; Accepted 10 July 2019
Available online 15 July 2019
0378-5173/

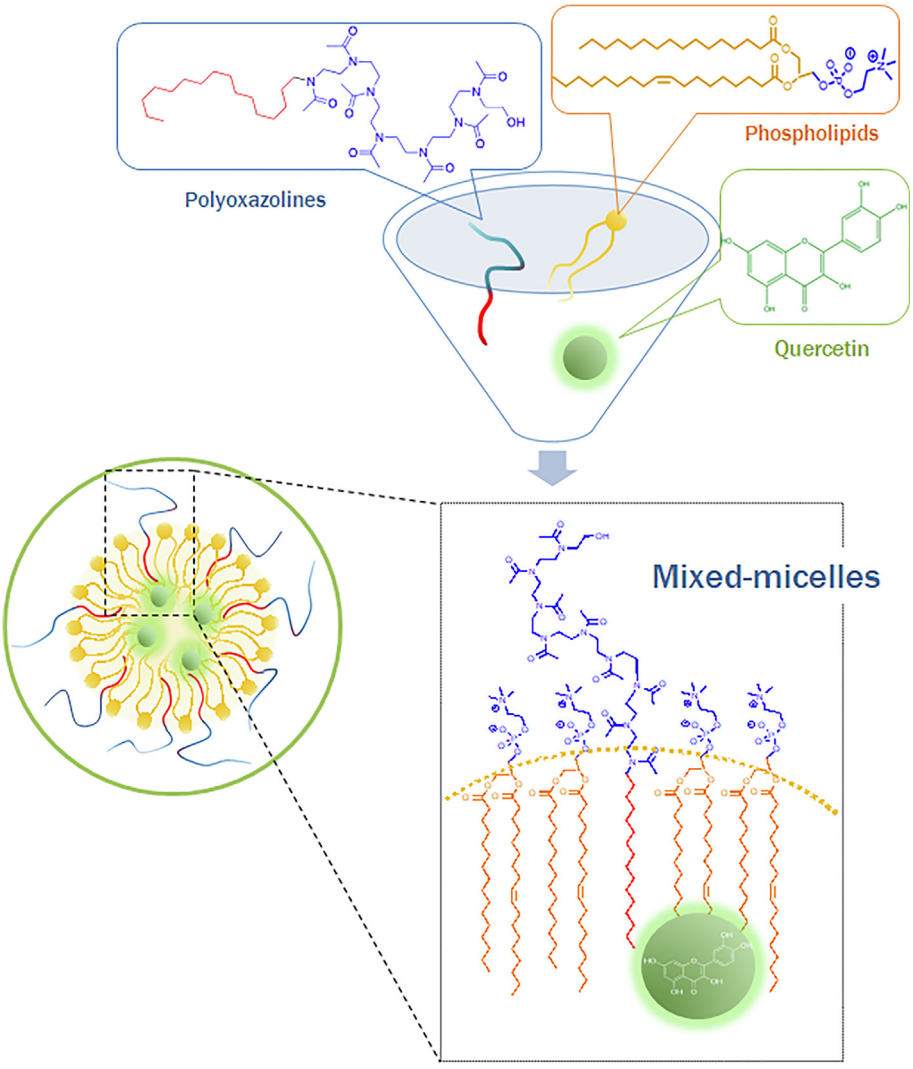

Scheme 1. Schematic representation of the mixed-micelles loaded with quercetin.

body tissues (Rudmann et al., 2013; Viegas et al., 2018).

Therefore, researchers as well as companies are trying to find a polymer alternative to PEG. In this context, the poly(2-R-2-oxazoline)s (POx)s are investigated as one of the most suitable candidates. This polyamide family can be regarded as analogous of poly(amino acid)s with pseudo-peptidic structure. The biomedical properties of POx have been largely described in recent publications (Hoogenboom, 2009; Adams and Schubert, 2007) or Lorson et al. (2018). Its biocompatibility (Goddard et al., 1989), excellent cytocompatibility (Bauer et al., 2012) and hemocompatiblity (Leiske et al., 2017) as well as the absence of accumulation in tissues and the rapid clearance from the bloodstream (Gaertner et al., 2007) have been emphasized. Moreover, the stealth behavior with suppression of the interactions with proteins and the immune system was proved (Zalipsky et al., 1996) allowing an immunocamouflage (Kyluik-Price et al., 2014). The most significant advance in biomedical POx concerns the recent results of Serina Therapeutics Inc. against Parkinson's disease (Moreadith et al., 2017). They validated phase I clinical trials on POx based rotigotine conjugates whereas multi-dose trials are currently in progress to phase II.

Moreover, the versatility of POx can be noted with an easy additional functionalization when compared to PEG regarding the R pendent groups along the backbone (Verbraeken et al., 2017; Guillerm et al., 2012b; Guillerm et al., 2012a; Korchia et al., 2015). Consequently, hydrophilic POx can be designed with methyl or ethyl R groups by contrast to hydrophobic POx with longer alkyl chains. Concerning poly(2-methyl-2-oxazoline), its more hydrophilic character than PEG and poly(2-ethyl-2-oxazoline) (Huber et al., 2008), offers an opportunity to elaborate amphiphilic (co)polymers contrasting with the hydrophobic block. In this way, to generate amphiphilic polymers, POx were associated with various hydrophobic blocks such as saturated or unsaturated lipids including fatty alcohols (El Asmar et al., 2016), fatty acids, triacyl glycerols (Stemmelen et al., 2013; Giardi et al., 2009) or phospholipids (Purrucker et al., 2004).

With the aim of protecting active pharmaceutical ingredients (API)s, several types of nanocarriers based on POx physically incorporating an API have been described. These formulations include solid dispersions, nanoparticles and micelles in which various APIs (paclitaxel, curcumin, doxorubicine) have been solubilized (Lorson et al., 2018). They were shown to be particularly interesting due to the limited number of steps required to synthesize the POx and the absence of necessity to tune the polymer towards the API as it is required for polymer-drug conjugates.

Regarding the association of POx and antioxidant API, little is reported in the literature. One can mention the conjugation of superoxide dismutase (SOD1) enzyme with POx to increase the release through the blood brain barrier and destroy superoxides (Yi and Kabanov, 2013). A radical fullerene-POx trap making use of the hydrophilicity of POx to disperse the anti-radical C60 molecules was also reported (Nukolova et al., 2011). A tribloc copolymer (PMeOx-*b*-PDMS-*b*-PMeOx) in polymersomes was shown to entrap a photosensitizer (rose bengal dye conjugated to bovine serum albumin) generating increased level of ROS

by photodynamic therapy (Baumann et al., 2014; Lorson et al., 2018).

To our knowledge, no POx topical formulation of flavonoids has been developed yet. In this context, a mixed nanosystem of POx and phospholipids for topical delivery was considered in this paper. Indeed, this hybrid system combines the features of liposomes and polymersomes by mixing the two components, i.e. the lipids and the amphiphilic copolymers, in a single vesicle. Either called hybrid polymer/lipid vesicle (Le Meins et al., 2013) or mixed micelles (Almgren, 2000), these systems have been studied over the past years and attracted attention for their versatile structure. It is notable that this mixture of lipid and polymer can lead to different nanostructures (D'Souza and Shegokar, 2016), such as core–shell of polymers and lipids (Mandal et al., 2013). Pippa *et al* have already worked on such hybrid nanosystems with POx and phospholipids for drug delivery systems and proved their efficacy as nanocontainers for the incorporation of therapeutic molecules (Pippa et al., 2013).

Herein, the investigated mixed-micelles were created based on phosphatidylcholine stabilized by an amphiphilic poly(2-methyl-2-oxazoline) bearing a long alkyl chain (Scheme 1). The stability and cell viability of these formulations were studied before and after being loaded with quercetin antioxidant. Then, the antioxidant activity of the loaded mixed micelles was measured. This work also aims to evaluate the potency of POx as an alternative to PEG in formulations.

2. Materials

2-Methyl-2-oxazoline (MOx, Sigma Aldrich, 99.0%) was dried over CaH_2, distilled at reduced pressure and stored under nitrogen atmosphere. Iodo-hexadecane (95.0%), potassium hydroxide (KOH), quercetin (95% HPLC), phosphatidylcholine (L-α-Phosphatidylcholine from egg yolk ≈ 60%), Brij®58, DPPH (2.2-diphenyl-1-picrylhydrazyl), phenazine methosulfate (PMS), *tert*-Butyl hydroperoxide solution (TBHP) 70% in water, acetonitrile, diethyl ether, methanol, acetone, phosphoric acid and 2,7-dichlorofluorescein diacetate (DCFDA) were purchased from Sigma Aldrich (Sigma Aldrich, Germany). Tween 80 (polysorbate 80) was purchased from BASF (BASF, Germany) and 3-(4,5-dimethylthiazol-2-yl)-5-(3-carboxymethoxyphenyl)-2-(4-sulfophenyl)-2H-tetrazolium, (MTS) from Promega (Promega, USA). MilliQ water was obtained from Milli-Q Gradient A10 (Merck Millipore, Germany) apparatus.

Chloroform (for HPLC stabilized with ethanol) was bought from Carlo-Erba (Carlo Erba Reagent, Spain). All the reagents were used without further purification.

Spectra/Por 6 dialysis membranes pre-wetted RC tubing with 0.5–1 kDa MWCO were purchased from Spectrum Labs (Spectrum Labs, USA).

3. Methods

3.1. Amphiphilic polyoxazolines synthesis (POx)

POx synthesis was performed by cationic ring-opening polymerization of MOx. The polymerization was achieved under a nitrogen atmosphere after dissolving iodo-hexadecane (3.564 g, 10.1 mmol) and MOx (15 eq, 151.7 mmol) in dry acetonitrile (0.5 M). The solution was vigorously stirred at 80 °C for 8 h and then quenched by addition of potassium hydroxide dissolved in methanol (5 eq, 50.5 mmol, 5 M). The solution was stirred at 40 °C for additional 8 h. The resulting polymer was isolated by precipitation by dropwise addition in cold diethyl ether and then filtration. The POx was then dialyzed with the dialysis membrane to eliminate residual diethyl ether and salts.

3.2. Chemical characterization of POx

Proton nuclear magnetic resonance (^{1}H NMR) spectra were recorded in $CDCl_3$ a Bruker 400 MHz spectrometer. The POx exhibited the following shifts (δ) in reference to residual $CHCl_3$ (δ = 7.26 ppm), where (s) stands for singlet, (d) doublet, (t) triplet, (m) multiplet: δ = 3.7–3.2 (m, (4n + 2)H, CH_2 POx and CH_2Nalkyl chain), 2.4–2.1 (m, 3n, CH_3 POx), 1.3 (m, 20H, CH_2 aliphatic), 0.9 (t, 3H, CH_3 aliphatic).

3.3. Critical aggregation concentration determination

The critical aggregation concentration (CAC) of the POx was determined by surface tension measurements using the Wilhelmy plate method on K100 Krüss Processor Tensiometer from Krüss GmbH. A concentration range of polymer from 0.001 to 400 mg/L was prepared in MilliQ water. Prior to measurements, the solutions were kept under gentle stirring for 24 h. Data were collected at 25 °C, a detection speed of 6 mm/min, detection sensitivity of 0.01 g and immersion depth of 2 mm using the Kruss software. A blank measurement was first performed using MilliQ water to ensure goodness of measure (γ = 69–73 mN).

3.4. Preparation of quercetin loaded mixed micelles (Q-MM)

The mixed micelles (MM) were obtained by the thin film method developed by Bangham (Bangham et al., 1967). First phosphatidylcholine (PC), polyoxazolines (POx) and quercetin (Q) were dissolved in a mixture of chloroform:acetone in 1:1 ratio, followed by the formation of thin film by evaporation of the solvent under vacuum. The film of mixed PC, POx and Q was hydrated by addition of filtered phosphate buffered saline (PBS, 150 mM, pH 7.4). Nanosized MM were obtained following a high pressure homogenizer process of 5 cycles at 10 000 PSI. Blank mixed micelles (B-MM) were prepared by the same method, except that quercetin was removed from the process.

Various molar ratios of Q: POx: PC were investigated from 3:1:10 to 7:1:50, after which the molar ratio 5:1:40 was selected. It was optimized to ensure the smallest and most stable MM, with the lowest POx amount and the highest drug loading of quercetin.

3.5. Photon correlation spectroscopy and electrophoretic mobility measurement

Hydrodynamic diameter and polydispersity index (PDI) were measured using a Zetasizer NanoZS apparatus (Malvern Instruments, UK) equipped with a He-Ne laser (wavelength: 632.8 nm) at a temperature of 20 °C and a scattering angle of 173° for detection. Zeta potential was measured with 1000 µL of mixed micelles in disposable capillary cell (Malvern Instruments, UK). All the results are the average of three independent measurements.

3.6. Stability of Q-MM

Blank and loaded MM samples were prepared and stored up to a month for stability study either at 4, 25 and 37 °C for B-MM and at 4 °C only for Q-MM. The stability was evaluated from particle size and PDI measurements (see Section 3.5) at day 0, 7, 14, 21, 28 for each temperature. The measurements were performed without filtration before measurements.

The stability of loaded mixed micelles was also evaluated using the concept of *in vitro* release by studying the concentration of quercetin diffusing through a nitrocellulose dialysis membrane from Q-MM to a receptor medium. The dialysis membrane was a 12–14 MWFC Spectra/Pore dialysis membrane (Spectrum laboratories, INC USA) and the receptor medium was composed of 40 mL PBS at pH 7.4 with 2 mass percent of Tween 80. The Q-MM were pre-filtered through 0.2 µm syringe filter (Whatman) to remove aggregated quercetin and then 3 mL were incorporated into the membrane. The stability was determined at 25 °C after 1, 2, 3, 4, 5, 6 and 7 h. Quercetin concentration was determined by HPLC (Section 3.9).

3.7. Transmission electron microscopy

Transmission electron microscopy was performed on TEM Jeol 1400 PLUS (Jeol. Ltbd, Tokyo, Japan) associated with a camera Jeol 2 K/2K. The samples previously diluted 10 times were deposited on grids type Cu formvar carbon and negatively stained with an aqueous uranyl acetate solution.

3.8. Differential scanning calorimetry (DSC)

The crude quercetin powder and lyophilized Q-MM were analyzed by DSC using a Perkin Elmer DSC400 apparatus (Perkin Elmer, USA).

The thermograms were recorded from 0 to 360 °C with a heating rate of 5 °C.min^{-1}.

3.9. HPLC analysis

High Pressure Liquid Chromatography (HPLC) analysis of quercetin was performed on LC6-2012HT apparatus (Shimadzu, Kyoto, Japan) using a Prontosil C18 column (120-5-C18 H5.0 µm, 250 × 4.0 mm) as stationary phase. The mobile phase was composed by a 40/60 vol ratio of acetonitrile to phosphoric acid solution at 0.2% by mass at pH = 1.9. The injection volume was 10 µL and the flow rate was kept constant at 1 mL·min^{-1} during the 10 min of analysis. The detection was achieved using a UV-vis detector, (Shimadzu, Kyoto, Japan) at 368 nm (Yang et al., 2009). The calibration curve was performed with solutions of quercetin in methanol from 1 µg/mL to 100 µg/mL with a good linearity (r^2 = 0.9999).

The stability of quercetin in aqueous medium receptor (Section 3.6) was established using a calibration curve of quercetin made in PBS buffer at pH 7.4 and Tween 80 (2% by mass) from 0.1 to 4 µg/mL (r^2 = 0.9996). The mobile phase, flow rate and detection wavelength remained unchanged.

3.10. Encapsulation efficacy (EE) and drug loading capacity (DL)

Quercetin loading capacity (DL) and encapsulation efficacy (EE) were determined by HPLC analysis as previously described (Section 3.9) using 50 µL of the Q-MM sample solubilized in 950 µL methanol.

The amount of quercetin loaded (Eqn. 1) and the encapsulation efficacy (Eqn. 2) were calculated using the following equations:

$$Drug\ loading\ (\%) = \frac{[mass\ of\ quercetin]}{[total\ mass]} \times 100 \quad (1)$$

$$Encapsulation\ efficacy\ (\%) = \frac{[amount\ of\ encapsulated\ quercetin]}{[amount\ of\ quercetin\ initially\ loaded]} \times 100 \quad (2)$$

3.11. In vitro radical scavenging ability by 2.2-diphenyl-1-picrylhydrazyl (DPPH°)

The antioxidant activity of Q-MM loaded with quercetin was investigated by looking at the reactivity of quercetin with the free radical 2.2-diphenyl-1-picrylhydrazyl (DPPH°) (Blois, 1958). The antioxidant activity was determined by UV-visible spectroscopy from the decrease of the DPPH° radical absorbance at 517 nm using the following DPPH° scavenging equation (Eqn. 3):

$$DPPH°\ scavenging\ (\%) = \frac{Absorption\ of\ control - Absorption\ of\ sample}{Absorption\ of\ control} \times 100 \quad (3)$$

In which *absorption of control* corresponds to the absorbance of 100 µM DPPH° solution. For the antioxidant activity test, the concentration of quercetin in Q-MM was set well below that of DPPH° at 2.5; 5; 7.5; 10; 12.5; 15 µM.

3.12. Cell culture

Mice fibroblasts cell line (NIH3T3) was purchased from American Type Cell Culture organization (USA). Cells were maintained in Dulbecco's Modified Eagle Medium (DMEM) (Gibco) supplemented with 10% fetal bovine serum (Life Technologies), 1% L-glutamine and 1% penicillin/streptomycin equivalent to final concentration of 2 nM for glutamine, 100 U·mL^{-1} for penicillin and 100 µg·mL^{-1} for streptomycin and incubated at 37 °C in humidified 5% CO_2.

3.13. Cell viability

NIH3T3 cells were seeded at 20,000 cells/cm^2 in 96 well plate and incubated for 24 h at 37 °C, 5% CO_2 to allow cell adhesion. POx and Brij®58 at 40 g/L were solubilized in DMEM supplemented medium and filtered through 0.2 µm (no mass was lost through filtration).

Cells were treated or not (control) with POx or with the PEG reference (Brij®58) solutions at a concentration range from 0.01 to 20 g/L. After 24 h of exposure, a CellTiter 96® Aqueous Non-Radioactive Cell Proliferation Assay (Promega, USA), was used to evaluate the cell viability following the manufacturer's instructions. The absorbance was then recorded at 490 nm using Multiskan™ GO Microplate Spectrophotometer (Thermo Scientific™, Waltham, Massachusetts, USA) and the background corresponding to wells free of cells (mean of 3) was subtracted from each triplicate mean. Values of treated cells were normalized to non-treated cells (representing the 100% cell viability).

Influence of a 24 h treatment with B-MM, crude quercetin, or Q-MM solutions was also performed following the same protocol with quercetin concentrations of 1, 5, 10, 25, 50 µg/mL. The absorbance background of the formulations without cells was subtracted to the cellular tests.

3.14. Antioxidant effect of quercetin on NIH3T3 cells

NIH3T3 cells were seeded at 20,000 cells/cm^2 in a 96 well black plate with clear bottom (Corning® Massachusetts, USA) and incubated 24 h at 37 °C, 5% CO_2 to allow cell adhesion. Then B-MM, crude quercetin, or Q-MM at a quercetin concentration of 5 µg/mL were added and incubated for another 24 h in supplemented DMEM. Cells were washed twice with PBS before addition of 200 µL of 2,7-dichlorofluorescein diacetate (DCFDA) reagent (20 µM in DMEM without phenol red). A serum free media was used to avoid deacetylated the DCFDA from serum esterases into a non fluorescent compound, which can later be oxidized by ROS into DCF resulting in erroneous data.

After 30 min incubation at 37 °C, 5% CO_2, cells were washed with PBS and placed in 200 µL DMEM without phenol red. A solution of *tert*-Butyl hydroperoxide (TBHP) (500 µM in PBS) was then added and the cells were incubated for 30 additional minutes. The fluorescent signal of dichlorofluorescein (DCF) generated by the reaction of DCFDA reagent with ROS was then measured (λexc 485 nm, λem 535 nm) using Tristar LB941 Spectrofluorimeter (Berthold Technologies, Germany). Values of treated cells were normalized to non-treated cells (representing the cells with 100% ROS intensity).

3.15. Statistical analysis

The statistical analysis of the data resulting from the cell viability and the antioxidant effect on cells was conducted with OriginPro software 8.1 (OriginLab, USA). A one-sample *t*-test with equal variance was performed to compare cell viability or antioxidant effect with formulations to viability of untreated cells (100%). A two-sample *t*-test with unequal variances was carried out to compare cell viability of formulations two by two. The P value reflects the significance with

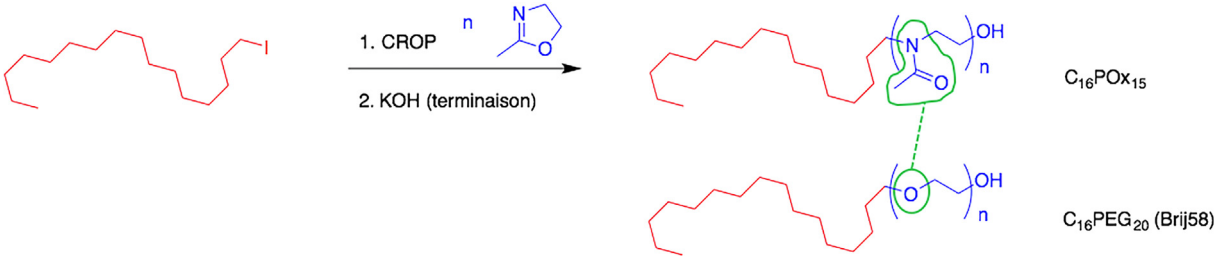

Scheme 2. Synthetic route of $C_{16}POx_{15}$ and structure of the Brij®58 used as a reference.

* = P < 0.05, ** = P < 0.01 and *** = P < 0.001.

4. Results

4.1. Synthesis of amphiphilic POx

Amphiphilic POx considered as nonionic surfactants were synthesized from iodide initiators and potassium hydroxide as terminating agent (Scheme 2). The hydrophilic lipophilic balance (HLB) of the polymers depends on the length of the POx block predefined by the initial monomer/initiator molar ratio. In our case, 1-iodohexadecane was employed to elaborate $C_{16}POx_{15}$ with narrow dispersity. The nonionic surfactant was well characterized by ^{1}H NMR spectroscopy with typical signals related to terminal CH_3 unit of hydrophobic block at 0.85 ppm and the CH_2 of POx block at 3.2–3.7 ppm (see Supplementary Fig. 1). The integration of these signals corresponds to the average degree of polymerization representing the length of the POx block, in our case 15, resulting in a molecular mass of the amphiphilic POx of 1520 g/mol and the measured critical aggregation concentration (CAC) of ~100 mg/L (66 µM).

The chemistry of POx platform looks like the one of PEG using a ring-opening process of polymerization from cyclic monomer, 2-R-2-oxazoline for POx and ethylene oxide for PEG. However, the polymerization process differs for oxazolines with a cationic ring-opening polymerization (CROP) whereas for ethylene oxide an anionic one occurs. It should be noted that the high toxicity of ethylene oxide, gaseous at room temperature, required specific equipments and cautious handling which is not the case for oxazolines. To evaluate some of the POx surfactant properties, PEG surfactant named Brij®58 (reference) was selected based on its similar alkyl chain length (molar mass of 1125 g/mol) inducing an almost similar CAC (90 mg/L vs. 100 mg/L) as it is the driving force of the self-assembly.

The surfactant properties of amphiphilic polymers in water were estimated by tensiometry measurements using the Wilhelmy plate method (Padday and Russell, 1960). It allows determining the critical aggregation concentration (CAC) value of surfactive molecules from the inflexion point occurring between a rapid decrease of surface tension at low concentrations and an almost constant value of the surface tension at higher concentrations. The CAC of $C_{16}POx_{15}$ was thus estimated at 100 mg/L (65.9 µmol/L) (data not shown) at 25 °C.

4.2. POx toxicity on NIH3T3 cells in comparison with PEG reference

The influence of POx ($C_{16}POx_{15}$) versus PEG reference (Brij®58) for a 24 h treatment on NIH3T3 cell viability was conducted by treating cells with increasing concentrations from 0.01 to 20 g/L (Fig. 1). Results were normalized to non treated cells (representing 100%).

For concentrations ranging from 0.01 to 0.5 g/L no significant cell viability decrease was observed for both POx ($C_{16}POx_{15}$) and PEG reference ($C_{16}PEG_{20}$). By contrast, following a 0.1 g/L Brij®58 ($C_{16}PEG_{20}$) treatment, cell viability fell to 32 ± 3% versus 112 ± 8% for POx ($C_{16}POx_{15}$). A decrease of cell viability was observed for POx ($C_{16}POx_{15}$) to 60 ± 5% only at 0.5 g/L. To summarize, following treatment from 0.1 to 0.2 g/L, POx has significantly (P < 0.001) less impact on cell viability than PEG reference. Interestingly, $IC_{50\ (cellular\ viability)}$ of the PEG amphiphilic reference was estimated at 0.090 g/L versus 0.75 g/L for amphiphilic POx.

4.3. Particle size and surface charge of mixed micelles

MM composed of PC and POx, with or without quercetin, were produced by thin film method and a high pressure homogenizer process (HPH) (Barnadas and Sabes, 2003). Table 1 summarizes the average particle size and zeta potential of B-MM and Q-MM. The loading of the MM with quercetin did not influence their diameter with a particle diameter of 19 ± 2 nm (Q-MM) instead of 18 ± 2 nm without quercetin (B-MM). It can be noted that, no light scattering from crude quercetin, which tends to aggregate from 2.5 µg/mL in PBS, was observed in Q-MM solutions. The zeta potential for both blank and loaded MM was measured at 0 mV, indicating that the formulations had no charge at the surface.

4.4. Morphology of mixed micelles

The morphology of MM was investigated by transmission electron microscopy. Fig. 2 shows typical images for Q-MM. Both B-MM and Q-MM exhibit a spherical shape and a similar size of about 20–30 nm. This is in agreement with the diameter of particles obtained from DLS analysis (Table 1).

4.5. DSC analysis of Q-MM

The crystallinity of quercetin as powder and once formulated in Q-MM was evaluated by differential scanning calorimetry, as illustrated in Fig. 3. Before the Q-MM measurement, the formulation was concentrated twice and lyophilized. The crude quercetin exhibited two peaks, one at 155 °C and 323 °C, which are consistent with the literature. The first one is due to water evaporation (Pool et al., 2012) and the second one results from melting of the quercetin (Sahoo et al., 2011). The glass transition of POx only appears at 37 °C (Supplementary Fig. 2). It is interesting to note that this glass transition was not observed on the Q-MM thermogram. More importantly, no peak for the quercetin crystallization could be observed. This indicates that nano-objects possess amorphous character, probably resulting from an homogeneous distribution of quercetin in the mixed micelle core.

The difference of quercetin structure revealed by DSC was also observed on NIH3T3 mice fibroblasts cells 24 h after addition of the Q-MM and the crude quercetin to the cells. The quercetin concentration was equivalent in both experiments (50 µg/mL). Optical microscopy clearly revealed the presence of needles on NIH3T3 with quercetin only (Fig. 4). Those were missing with Q-MM, i.e. once quercetin has been loaded in mixed micelles (Fig. 4). This argues in favor of an homogenous distribution of quercetin in MM.

4.6. Formulation stability studies of B-MM and Q-MM

The formulation stability of the B-MM was assessed over a month and evaluated every week at 4, 25 and 37 °C by analyzing the

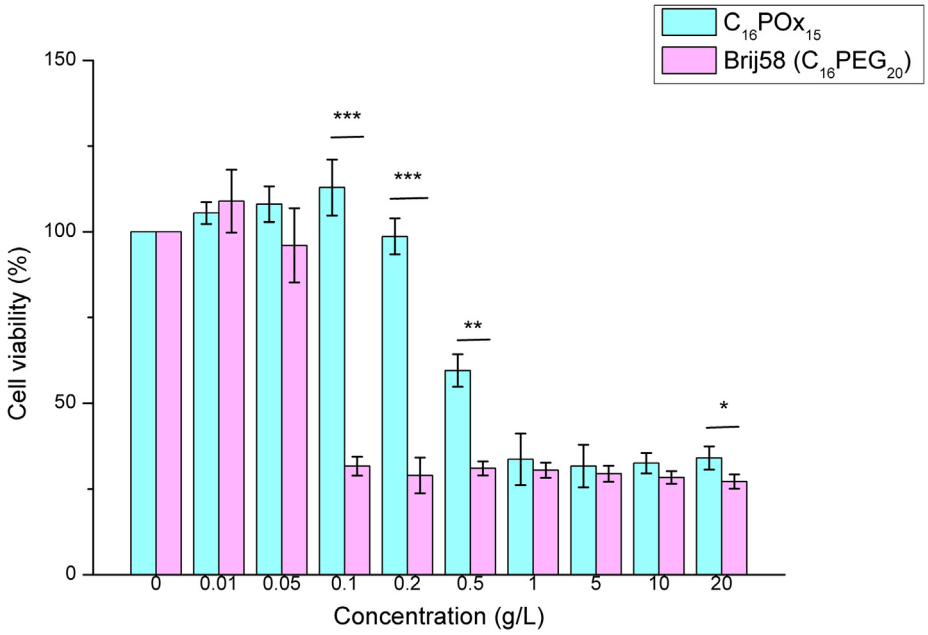

Fig. 1. Cell viability of mice fibroblast NIH3T3 co-incubated with increasing concentration of amphiphilic POx ($C_{16}POx_{15}$) compared to amphiphilic PEG surfactant Brij® 58 ($C_{16}PEG_{20}$) for 24 h (n = 3). Statistical analysis was performed by a two-sample *t*-test between POx and PEG values (*P < 0.05, **P < 0.01 and ***P < 0.001).

Table 1
Mixed micelles structure characteristics.

Formulations	B-MM	Q-MM
Particle diameter (nm)	18 ± 2	19 ± 2
PDI	0.30 ± 0.02	0.28 ± 0.01
Zeta potentiel (mV)	0.05 ± 0.08	0.03 ± 0.05

hydrodynamic diameter and polydispersity index (PDI) of MM using DLS experiments as shown in Fig. 5. The B-MM remained stable over a month at each temperature. For example, at 37 °C, only a slight size increase from 24 nm to 31 nm with a PDI ≤ 0.3 was observed, thus indicating the good stability of the nano-formulations upon time and temperature.

As quercetin is very sensitive to thermal degradation, the Q-MM stability study was conducted at 4 °C only. The particles were also stable over 14 days with no variation of the particle size from 26 nm on day 0 to 25 nm on day 28 with a PDI remaining close to 0.3.

The stability of the Q-MM has also been evaluated through the release of quercetin over time, which should happen after decomposition on skin before the formulation had penetrated in the epidermis. To this end, a suspension of Q-MM was dialyzed in PBS buffer and in presence of Tween 20 (2% by masss) for 7 h. A slight release of quercetin of only 6% was observed after 7 h of dialysis (Supplementary Fig. 3), confirming the above mentioned stability of the quercetin encapsulated MM formulations.

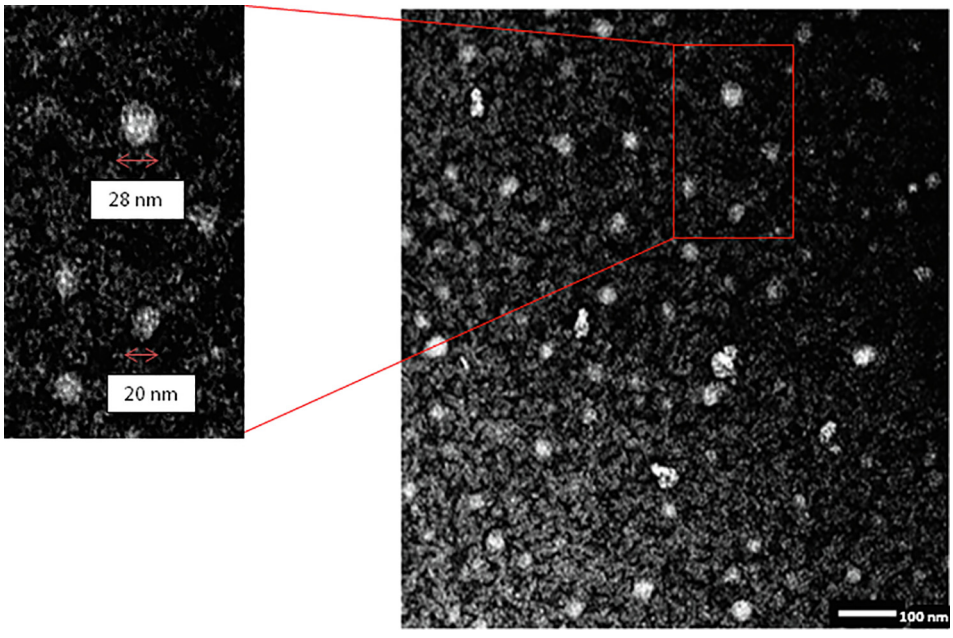

Fig. 2. TEM images for Q-MM.

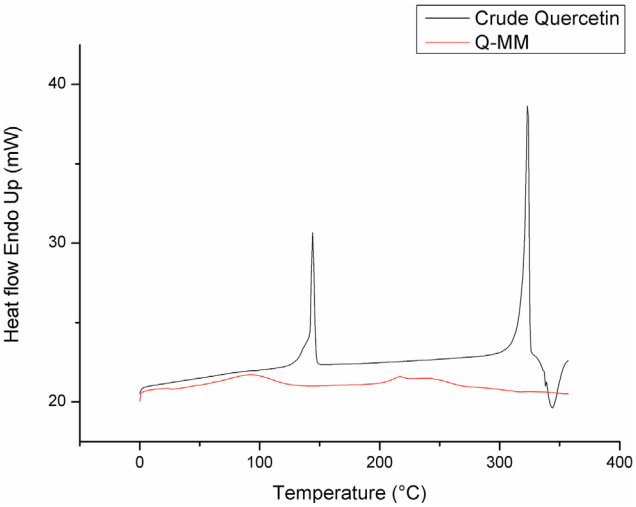

Fig. 3. Thermograms properties of crude quercetin and Q-MM.

4.7. Drug loading (DL) and encapsulation efficacy (EE) of Q-MM

The drug loading (DL) and encapsulation efficiency (EE) for quercetin in Q-MM were calculated from HPLC analysis using the Eqs. (1) and (2) described in Section 3.10. DL reflects the amount of loaded quercetin relative to the total mass of the MM formulation, whereas EE represents the amount of quercetin experimentally encapsulated by comparison with the amount of quercetin added in solution. DL for this dermal delivery system was evaluated to 3.6 ± 0.2% corresponding to an EE of 94 ± 4%.

4.8. Mixed micelles cellular viability on NIH3T3

The cell viability test was performed on mice fibroblasts (NIH3T3) co-incubated with crude quercetin, B-MM and Q-MM at concentrations ranging from 1 to 50 µg/mL (Fig. 6). Results were normalized to non-treated cells (representing 100%). After 24 h, crude quercetin treatment induced a decrease in cell viability reaching 72 ± 9% at quercetin concentration of 10 µg/mL. By contrast no significant decrease in cell viability was observed when cells were treated with B-MM, at all concentrations. Interestingly, the quercetin encapsulated in MM showed less toxicity than the crude antioxidant at equivalent concentration of quercetin. For example at 25 µg/mL, the crude quercetin cell viability was determined at 33 ± 17% and the one for Q-MM was twice higher at 65 ± 8%. The $IC_{50\ (cellular\ viability)}$ was determined at 17.5 µg/mL for crude quercetin and 37.5 µg/mL for Q-MM evidencing a lower impact of quercetin on cell viability once encapsulated in Q-MM.

4.9. Antioxidant effect

4.9.1. In vitro radical scavenging ability of Q-MM

The radical scavenging ability of the crude quercetin and Q-MM was investigated with *in vitro* test using 2.2-diphenyl-1-picrylhydrazyl (DPPH°) as a radical source. The quercetin antioxidant reacts with the free radical located at the hydrazine position of the DPPH°, thus leading to the reduced hydrazine form (DPPHH) and decreasing the amount of radicals. The DPPH test allowed to determine the $IC_{50\ (DPPH^{\circ}\ inhibition)}$ value: the concentration of quercetin for which 50% of the DPPH° reacted. Fig. 7 illustrates the DPPH° inhibition with quercetin

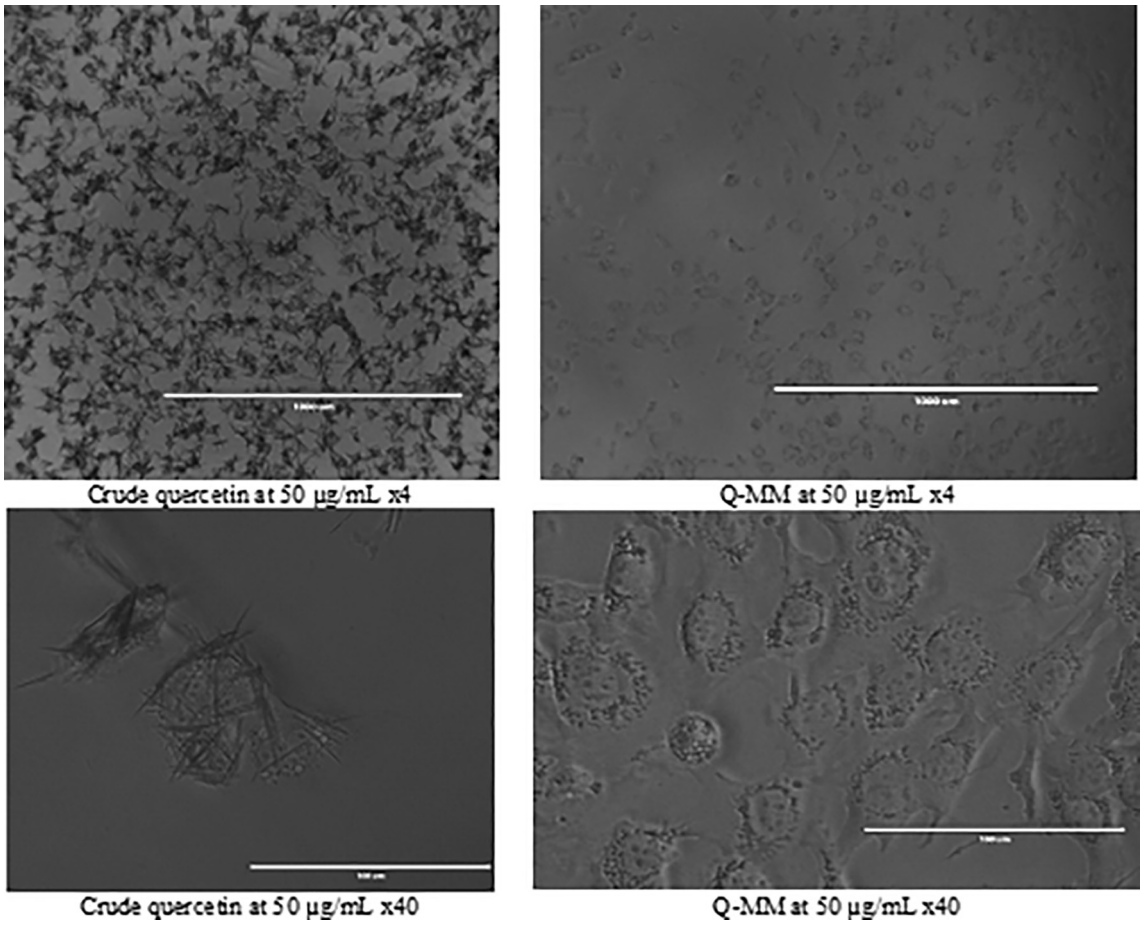

Fig. 4. Optical microscopy images of crude quercetin and Q-MM on NIH3T3 cells.

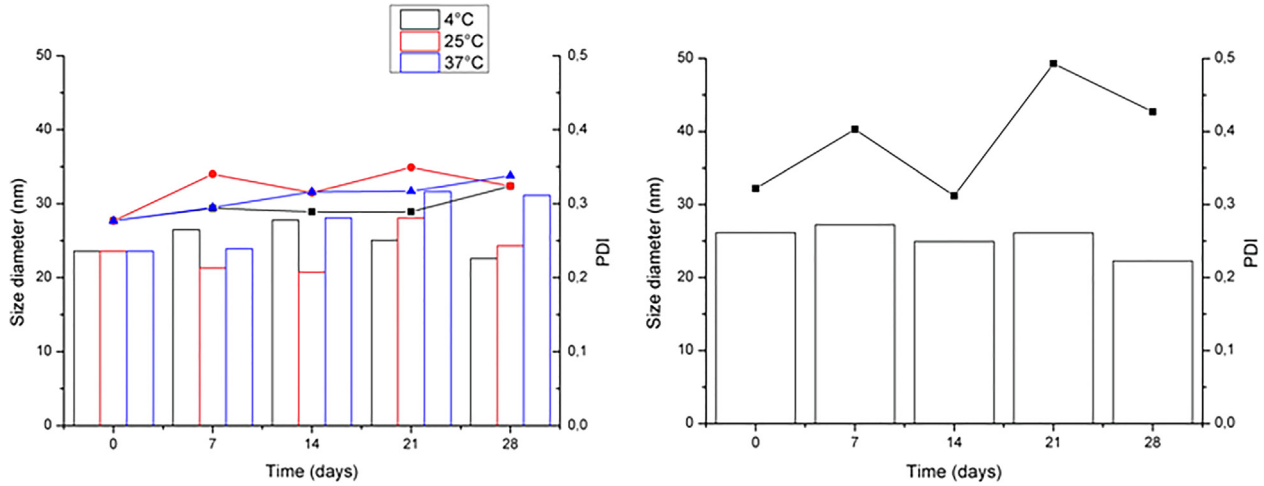

Fig. 5. Particle size (column) and PDI (symbols) of B-MM at 4, 25, 37 °C (left) and Q-MM at 4 °C (right) over a month (n = 3).

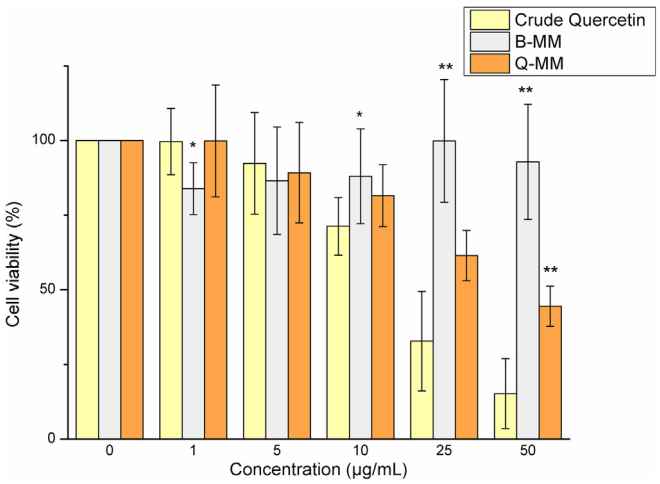

Fig. 6. Cell viability of mice fibroblasts (NIH3T3) co-incubated with crude quercetin, B-MM and Q-MM for 24 h (n = 3). Statistical analysis was performed by a two-sample *t*-test between crude quercetin and B-MM, Q-MM (*P < 0.05, **P < 0.01).

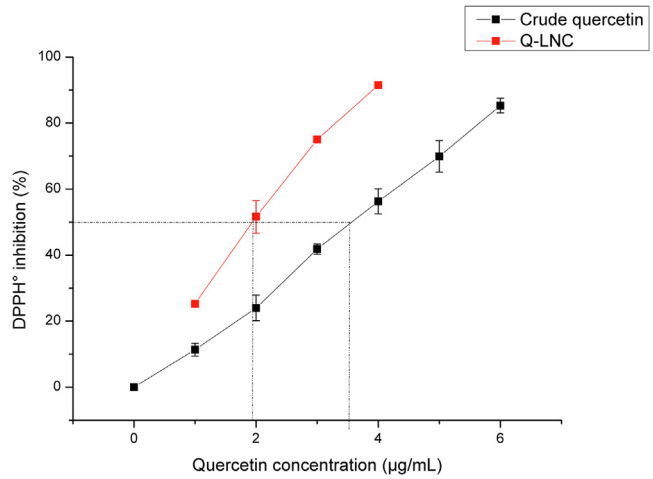

Fig. 7. DPPH° inhibition of free quercetin and Q-MM with quercetin concentration.

concentration ranging from 2.5 to 15 µM for the quercetin free and encapsulated in MM (Q-MM). The $IC_{50\ (DPPH^{\circ}\ inhibition)}$ values deduced from those measurements were 9 µM (3.6 µg/mL) for the free quercetin and 6.5 µM (2.6 µg/mL) for Q-MM. This indicates that the radical scavenging activity of quercetin was preserved upon encapsulation and even enhanced with respect to crude quercetin since its IC_{50} value was lower.

4.9.2. Cellular testing on NIH3T3 with TBHP

The antioxidant activity of the Q-MM was tested on mice fibroblasts (NIH3T3) in comparison with crude quercetin and B-MM (Fig. 8). A quercetin concentration of 5 µg/mL was selected as no decrease in cell viability was observed regardless of the formulation.

Cells were first treated with formulations for 24 h before being washed and labeled with 2,7-dichlorofluorescein (DCFDA). The oxidative stress was then induced by *tert*-butyl hydroperoxide (TBHP) for 30 min before measuring the fluorescence intensity signal. A serum free medium was used to avoid deacetylated the DCFDA from serum esterases into a non fluorescent compound, which can later be oxidized by ROS into DCF resulting in erroneous data.

The results were normalized to TBHP treated cells (positive control) and the untreated cells were set as negative control. The addition of TBHP increased the ROS generated by 25 ± 2% (P < 0.001)

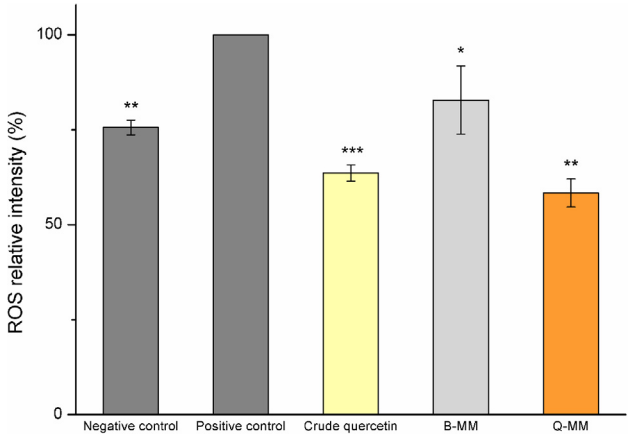

Fig. 8. ROS relative intensity for crude quercetin, B-MM and Q-MM (quercetin concentration 5 µg/mL) (n = 3). Negative control was untreated cells (without TBHP or formulations) and positive control was cells treated with TBHP without formulation. Fluorescent intensity was normalized to TBHP treated cells (positive control). A one sample *t*-test relative to positive control cells was performed (*P < 0.05, **P < 0.01 and ***P < 0.001).

compared to negative control. The crude quercetin and Q-MM formulation significantly reduced generated ROS by 36 ± 3% and by 42 ± 2% respectively compared to cells treated with TBHP. The antioxidant activity of the quercetin was maintained once formulated in MM. No significant difference in the antioxidant activity of crude quercetin versus Q-MM was evidenced.

Therefore Q-MM was able to scavenge the excess of ROS allowing a recovery to basal ROS concentration values. The antioxidant effect of the Q-MM seems to be only due to the quercetin encapsulated in the formulation as the ability of B-MM to reduce ROS was very low.

5. Discussion

Two aspects were investigated in this study: (i) the stability of mixed micelles formulated with POx as alternative to PEG and (ii) quercetin loading and quercetin antioxidant efficiency in these POx-formulations (Q-MM). Among all the previously developed formulations for topical delivery of quercetin (Hatahet et al., 2018), mixed micelles were selected as the first proof of concept for antioxidant POx-formulations. These formulations were constituted of phosphatidylcholine and an amphiphilic poly(2-methyl-2-oxazoline) molecule bearing a long alkyl chain (POx, $C_{16}POx_{15}$).

The surfactant property of POx itself was first evaluated. It presents a critical aggregation concentration (CAC) of ~100 mg/L, which is similar to structural analogue Brij®58 used as a reference. In contrast, the impact of the two amphiphilic molecules on cell viability was very different. A better cell viability in presence of POx (Fig. 1) was highlighted with a $IC_{50\ (cellular\ viability)}$ of 0.75 g/L compared to 0.09 g/L for Brij®58. The POx concentration for formulation of mixed micelles was about 50 times under the $IC_{50\ (cellular\ viability)}$ of POx, ensuring non toxic working conditions. Therefore, POx was proved to have significantly ($P < 0.001$) less impact on cell viability than its PEG equivalent. These results are consistent with the literature since the polyoxazolines polymer family is known to have an excellent cytocompatibility and hemocompatibility (Lorson et al., 2018). However, it is the first time that an amphiphilic POx with such architecture ($C_{16}POx_{15}$) was investigated. Then, this amphiphilic POx was associated with phospholipids to increase the solubility of hydrophobic antioxidant within the micelles. The mixed micelles of phosphatidylcholine stabilized by $C_{16}POx_{15}$ (B-MM) were produced using thin film process. After a high pressure homogenization, the formulation presented a reduced homogeneous particle size of 18 ± 2 nm (Fig. 2). These DLS and CAC results confirmed that nanosized mixed-micelles were created and not POx micelles and liposomes coexisting.

The same process was used in the presence of quercetin, leading to an excellent encapsulation efficiency that reached up to 94 ± 4%. This allowed a particularly high concentration of antioxidant in the formulations to be loaded (3.6 ± 0.2%), which reached 188 µg/ml in Q-MM instead of 2.48 µg/ml in PBS. It was shown that neither the spherical shape nor the particle size of MM were modified upon loading with quercetin (Q-MM) (Table 1). This contrasts with the existing hybrid nanosystems DPPC:MPOx (Pippa et al., 2013) for which the incorporation of indomethacin (with the same molar mass as quercetin and the same nature of polycyclic aromatic ring) induced a significant size increase. The incorporation efficiency was also significantly lower with a maximum of 17%. Looking at some others lipid formulations for topical delivery of quercetin the encapsulation efficiency, drug loading and particle size reached with the Q-MM (94%, 3.6%, 19 nm), are more satisfactory than nanostructured lipid carriers (89.95%, 3.05%, 215.2 nm) (Chen-yu et al., 2012), phospholipids based vesicles (48–75%, NV (no value), 80–220 nm) (Chessa et al., 2011), lecithin-chitosan nanoparticles (48.5%, 2.45%, 100 nm) (Tan et al., 2011), and nanovesicles (81–91%, NV, 80–110 nm) (Manca et al., 2014). Moreover, the nanometric size obtained for the MM formulation is particularly interesting since it is known to ensure enhanced penetration into skin (Schäfer-Korting et al., 2007).

Concerning the quercetin dispersion in Q-MM, a thermal analysis performed by DSC corroborated by microscopy (Fig. 4) indicated that quercetin was well dispersed in the core of Q-MM, losing its crystalline character in favor of an amorphous phase (Pool et al., 2012; Sahoo et al., 2011). This feature also indicates that once the Q-MM has penetrated into skin, quercetin should be easily released out of the formulation.

To evaluate POx formulation stability, the size and PDI of B-MM and Q-MM were measured every week at various temperatures (4, 25 and 37 °C) for 28 days. B-MM remained stable at all 3 temperatures reflecting the high stabilizing capacity of POx. Regarding Q-MM, since quercetin is very sensitive to thermal degradation (Wang and Zhao, 2016) even at 25 and 37 °C leading overtime to antioxidant degradation into intermediate products, the stability study was only conducted at storage condition 4 °C, as also performed by Bose et al (Bose et al., 2013). The size of Q-MM remained around 26 nm over 14 days with a PDI around 0.3. The PDI increase after 14 days might be due to the quercetin loading as it was not the case for B-MM. This formulation could be more stable once loaded with another active compound. MM thus represents a quite stable quercetin formulation as a low quantity of quercetin (< 6%) was released *in vitro* from the formulation over 7 h. All the results demonstrated the efficiency of POx to stabilize MM formulation and its ability to load a large amount of antioxidants such as quercetin, indicating this formulation is promising for topical application. Indeed, the lipid composition of the MM along with the presence of POx could facilitate the delivery of quercetin in the skin epidermis (Ashtikar et al., 2016; Casiraghi et al., 2015).

The cellular viability of crude quercetin, B-MM and Q-MM was evaluated on mice fibroblasts after 24 h of exposure. With a quercetin concentration from 10 to 25 µg/mL, cell viability dropped from 72 ± 9% to 33 ± 17% for crude quercetin whereas a slightler decrease for Q-MM (from 82 ± 10% to 62 ± 8%) was observed (Fig. 6). This evidenced the interest of quercetin in association with MM. This statement is also highlighted by difference in $IC_{50\ (cellular\ viability)}$ values, as crude quercetin has a value twice higher than Q-MM (17.5 µg/mL versus 37.5 µg/mL respectively). Moreover, it has been confirmed that the effect of Q-MM was only due to the quercetin itself as B-MM had no impact on cell viability. These results confirmed the cell viability study of polyoxazolines (Fig. 1) in which POx had no impact on cell viability over a broad concentration range including the one used for MM formulation (about 15 mg/L). MM formulations were concentrated enough in quercetin so their antioxidant efficacy could be evaluated.

The antioxidant activity of Q-MM related to crude quercetin was first evaluated *in vitro* using DPPH assay, to ensure that the radical scavenging activity of quercetin was preserved and was even enhanced once encapsulated. The $IC_{50\ (DPPH^{\circ}\ inhibition)}$ value of Q-MM compared to crude quercetin decreased from 9 to 6.5 µM (equivalent to 3.6 to 2.6 µg/mL). The Q-MM antioxidant capacity also relies on POx being more stable regarding oxidative degradation compared to PEG: the polyether backbone is more prone to oxidative degradation (Ostuni et al., 2001). To evaluate the ability of quercetin to counteract the oxidative stress induced by ROS, mice fibroblasts were used as a cellular model with an oxidative stress induced by TBHP. The antioxidant efficacy of the quercetin was maintained once encapsulated in Q-MM. By comparison, crude quercetin was able to reduced the ROS generated by TBHP by 36% whereas Q-MM decreased them by 42% (Fig. 8). Moreover, Q-MM was able to scavenge the excess of ROS allowing a recovery to basal ROS concentration values (about 75% as measured with untreated cells). Since the toxicity of Q-MM was lower than crude quercetin, the concentration for the antioxidant test could be increased for a potentially even higher efficacy on cells.

6. Conclusion

This study on amphiphilic polyoxazolines ($C_{16}POx_{15}$) provides insight into the great promise this polymer family holds for the

development of pharmaceutical and cosmetic formulations. The higher cell viability (at a similar CAC value) compared to Brij®58, a worldwide used industrial nonionic surfactant, demonstrates the potential of this POx family in the formulation of API. The ability of the amphiphilic POx to produce stable formulations was investigated for the first time with mixed micelles of POx and phosphatidylcholine using thin film and HPH process. DLS and TEM measurements showed spherical micelles of around 18 nm without API (B-MM) and no size increase once loaded in a natural antioxidant quercetin (Q-MM). These mixed-micelles were stable over 14 days and present a long-lasting encapsulation with < 6% release over 7 h. Moreover, a good quercetin encapsulation (94 ± 4%) efficiency was measured with these nanosystems allowing its homogeneous solubilization in the core under amorphous character. Therefore, Q-MM can be used as a reservoir of quercetin. Once loaded in the MM, the quercetin impact on cell viability was twice reduced while the quercetin antioxidant efficacy was preserved. Q-MM was able to reduce by 42% of the ROS generated by TBHP allowing a recovery to basal ROS concentration values.

Optimal features such as composition, size, stability, encapsulation efficiency, preservation of antioxidant activity are brought together in the mixed micelles, a very promising formulation for an effective topical delivery.

Declaration of Competing Interest

None.

Appendix A. Supplementary data

Supplementary data to this article can be found online at https://doi.org/10.1016/j.ijpharm.2019.118516.

References

Adams, N., Schubert, U.S., 2007. Poly(2-oxazolines) in biological and biomedical application contexts. Adv. Drug Deliv. Rev. 59, 1504–1520.

Almgren, M., 2000. Mixed micelles and other structures in the solubilization of bilayer lipid membranes by surfactants. Biochim. Biophys. Acta (BBA) – Biomembr. 1508, 146–163.

Andreia, A., Helena Margarida, R., Helena Cabral, M., Sandra, S., 2011. Topical delivery of antioxidants. Curr. Drug Deliv. 8, 640–660.

Ashtikar, M., Nagarsekar, K., Fahr, A., 2016. Transdermal delivery from liposomal formulations – evolution of the technology over the last three decades. J. Control. Release 242, 126–140.

Bangham, A.D., De Gier, J., Greville, G.D., 1967. Osmotic Properties and Water Permeability of Phospholipid Liquid Crystals.

Barnadas, R.R., Sabes, X.M., 2003. Liposomes prepared by high-pressure homogenizers.

Baudouin, C., Charveron, M., Tarroux, R., Gall, Y., 2002. Environmental pollutants and skin cancer. Cell Biol. Toxicol. 18, 341–348.

Bauer, M., Lautenschlaeger, C., Kempe, K., Tauhardt, L., Schubert, U.S., Fischer, D., 2012. Poly(2-ethyl-2-oxazoline) as alternative for the stealth polymer poly(ethylene glycol): comparison of in vitro cytotoxicity and hemocompatibility. Macromol. Biosci. 12, 986–998.

Baumann, P., Spulber, M., Dinu, I.A., Palivan, C.G., 2014. Cellular trojan horse based polymer nanoreactors with light-sensitive activity. J. Phys. Chem. B 118, 9361–9370.

Blois, M.S., 1958. Antioxidant determinations by the use of a stable free radical. Nature 181, 1199–1200.

Bose, S., Du, Y., Takhistov, P., Michniak-Kohn, B., 2013. Formulation optimization and topical delivery of quercetin from solid lipid based nanosystems. Int. J. Pharm. 441, 56–66.

Caddeo, C., Díez-Sales, O., Pons, R., Fernàndez-Busquets, X., Fadda, A.M., Manconi, M., 2014. Topical anti-inflammatory potential of quercetin in lipid-based nanosystems. In vivo and in vitro evaluation. Pharm. Res. 31, 959–968.

Casiraghi, A., Selmin, F., Minghetti, P., Cilurzo, F., Montanari, L., 2015. Nonionic surfactants: polyethylene glycol (PEG) ethers and fatty acid esters as penetration enhancers. In: Dragicevic, N., Maibach, H.I. (Eds.), Percutaneous Penetration Enhancers Chemical Methods in Penetration Enhancement: Modification of the Stratum Corneum. Springer Berlin Heidelberg, Berlin, Heidelberg, pp. 251–271.

Chen-yu, G., Chun-fen, Y., Qi-lu, L., Qi, T., Yan-wei, X., Wei-na, L., Guang-xi, Z., 2012. Development of a Quercetin-loaded nanostructured lipid carrier formulation for topical delivery. Int. J. Pharm. 430, 292–298.

Chessa, M., Caddeo, C., Valenti, D., Manconi, M., Sinico, C., Fadda, A.M., 2011. Effect of penetration enhancer containing vesicles on the percutaneous delivery of quercetin through new born pig skin. Pharmaceutics 3, 497–509.

D'Souza, A., Shegokar, R., 2016. Polymer: Lipid Hybrid Nanostructures in Cancer Drug Delivery: Successes and Limitations, pp. 431–463.

El Asmar, A., Gimello, O., Morandi, G., Le Cerf, D., Lapinte, V., Burel, F., 2016. Tuning the thermo-sensitivity of micellar systems through a blending approach. Macromolecules 49, 4307–4315.

Gaertner, F.C., Luxenhofer, R., Blechert, B., Jordan, R., Essler, M., 2007. Synthesis, biodistribution and excretion of radiolabeled poly(2-alkyl-2-oxazoline)s. J. Control. Rel. 119, 291–300.

Giardi, C., Lapinte, V., Charnay, C., Robin, J.J., 2009. Nonionic polyoxazoline surfactants based on renewable source: synthesis, surface and bulk properties. React. Funct. Polym. 69, 643–649.

Goddard, P., Hutchinson, L.E., Brown, J., Brookman, L.J., 1989. Soluble polymeric carriers for drug delivery. Part 2. Preparation and in vivo behaviour of N-acylethylenimine copolymers. J. Control. Release 10, 5–16.

Guillerm, B., Darcos, V., Lapinte, V., Monge, S., Coudane, J., Robin, J.-J., 2012a. Synthesis and evaluation of triazole-linked poly(ε-caprolactone)-graft-poly(2-methyl-2-oxazoline) copolymers as potential drug carriers. Chem. Commun. 48, 2879–2881.

Guillerm, B., Monge, S., Lapinte, V., Robin, J.-J., 2012b. How to modulate the chemical structure of polyoxazolines by appropriate functionalization. Macromol. Rapid Commun. 33, 1600–1612.

Hatahet, T., Morille, M., Hommoss, A., Devoisselle, J.M., Müller, R.H., Bégu, S., 2016a. Quercetin topical application, from conventional dosage forms to nanodosage forms. Eur. J. Pharm. Biopharm. 108, 41–53.

Hatahet, T., Morille, M., Hommoss, A., Devoisselle, J.M., Müller, R.H., Bégu, S., 2018. Liposomes, lipid nanocapsules and smartCrystals®: a comparative study for an effective quercetin delivery to the skin. Int. J. Pharm. 542, 176–185.

Hatahet, T., Morille, M., Hommoss, A., Dorandeu, C., Müller, R.H., Bégu, S., 2016b. Dermal quercetin smartCrystals®: formulation development, antioxidant activity and cellular safety. Eur. J. Pharm. Biopharm. 102, 51–63.

Hatahet, T., Morille, M., Shamseddin, A., Aubert-Pouëssel, A., Devoisselle, J.M., Bégu, S., 2017. Dermal quercetin lipid nanocapsules: influence of the formulation on antioxidant activity and cellular protection against hydrogen peroxide. Int. J. Pharm. 518, 167–176.

Hoogenboom, R., 2009. Poly(2-oxazoline)s: a polymer class with numerous potential applications. Angew. Chem. Int. Ed. 48, 7978–7994.

Huber, S., Hutter, N., Jordan, R., 2008. Effect of end group polarity upon the lower critical solution temperature of poly(2-isopropyl-2-oxazoline).

Korchia, L., Bouilhac, C., Lapinte, V., Travelet, C., Borsali, R., Robin, J.-J., 2015. Photodimerization as an alternative to photocrosslinking of nanoparticles: proof of concept with amphiphilic linear polyoxazoline bearing coumarin unit. Polym. Chem. 6, 6029–6039.

Krutmann, J., Bouloc, A., Sore, G., Bernard, B.A., Passeron, T., 2017. The skin aging exposome. J. Dermatol. Sci. 85, 152–161.

Kyluik-Price, D.L., Li, L., Scott, M.D., 2014. Comparative efficacy of blood cell immunocamouflage by membrane grafting of methoxypoly(ethylene glycol) and polyethyloxazoline. Biomaterials 35, 412–422.

Le Meins, J.F., Schatz, C., Lecommandoux, S., Sandre, O., 2013. Hybrid polymer/lipid vesicles: state of the art and future perspectives. Mater. Today 16, 397–402.

Leiske, M.N., Trützschler, A.-K., Armoneit, S., Sungur, P., Hoeppener, S., Lehmann, M., Traeger, A., Schubert, U.S., 2017. Mission ImPOxable – or the unknown utilization of non-toxic poly(2-oxazoline)s as cryoprotectants and surfactants at the same time. J. Mater. Chem. B 5, 9102–9113.

Lorson, T., Lübtow, M.M., Wegener, E., Haider, M.S., Borova, S., Nahm, D., Jordan, R., Sokolski-Papkov, M., Kabanov, A.V., Luxenhofer, R., 2018. Poly(2-oxazoline)s based biomaterials: a comprehensive and critical update. Biomaterials 178, 204–280.

Lubich, C., Allacher, P., de la Rosa, M., Bauer, A., Prenninger, T., Horling, F.M., Siekmann, J., Oldenburg, J., Scheiflinger, F., Reipert, B.M., 2016. The mystery of antibodies against polyethylene glycol (peg) – what do we know? Pharm. Res. 33, 2239–2249.

Manca, M.L., Castangia, I., Caddeo, C., Pando, D., Escribano, E., Valenti, D., Lampis, S., Zaru, M., Fadda, A.M., Manconi, M., 2014. Improvement of quercetin protective effect against oxidative stress skin damages by incorporation in nanovesicles. Colloids Surf., B 123, 566–574.

Mandal, B., Bhattacharjee, H., Mittal, N., Sah, H., Balabathula, P., Thoma, L.A., Wood, G.C., 2013. Core–shell-type lipid–polymer hybrid nanoparticles as a drug delivery platform. Nanomedicine: nanotechnology. Biol. Med. 9, 474–491.

Marks, J.G., Miller, J.J., 2019. 2 – Structure and Function of the Skin, in: Marks, J.G., Miller, J.J. (Eds.), Lookingbill and Marks' Principles of Dermatology (Sixth Edition). Content Repository Only!, London, pp. 2–10.

Martena, V., Hoti, E., Malaj, L., Di Martino, P., 2012. Permeation and skin retention of quercetin from microemulsions containing Transcutol® P AU – Censi, Roberta. Drug Dev. Ind. Pharm. 38, 1128–1133.

Moreadith, R.W., Viegas, T.X., Bentley, M.D., Harris, J.M., Fang, Z., Yoon, K., Dizman, B., Weimer, R., Rae, B.P., Li, X., Rader, C., Standaert, D., Olanow, W., 2017. Clinical development of a poly(2-oxazoline) (POZ) polymer therapeutic for the treatment of Parkinson's disease – Proof of concept of POZ as a versatile polymer platform for drug development in multiple therapeutic indications. Eur. Polym. J. 88, 524–552.

Nagula, R.L., Wairkar, S., 2019. Recent advances in topical delivery of flavonoids: a review. J. Control. Release 296, 190–201.

Nukolova, N.V., Oberoi, H.S., Cohen, S.M., Kabanov, A.V., Bronich, T.K., 2011. Folate-decorated nanogels for targeted therapy of ovarian cancer. Biomaterials 32, 5417–5426.

Ostuni, E., Chapman, R.G., Holmlin, R.E., Takayama, S., Whitesides, G.M., 2001. A survey of structure – property relationships of surfaces that resist the adsorption of protein. Langmuir 17, 5605–5620.

Padday, J.F., Russell, D.R., 1960. The measurement of the surface tension of pure liquids and solutions. J. Colloid Sci. 15, 503–511.

Pippa, N., Merkouraki, M., Pispas, S., Demetzos, C., 2013. DPPC:MPOx chimeric advanced Drug Delivery nano Systems (chi-aDDnSs): Physicochemical and structural characterization, stability and drug release studies. Int. J. Pharm. 450, 1–10.

B. Poljšak U. Glavan R. Dahmane Poljšak, B., Glavan, U., Dahmane, R., 2011. Skin Cancer, Free Radicals and Antioxidants.

Pool, H., Quintanar, D., Figueroa, J.d.D., Marinho Mano, C., Bechara, J.E.H., GodÍnez, L.A., Mendoza, S., 2012. antioxidant effects of quercetin and catechin encapsulated into PLGA nanoparticles. J. Nanomater. 2012, 12.

Purrucker, O., Förtig, A., Jordan, R., Tanaka, M., 2004. Supported membranes with well-defined polymer tethers—incorporation of cell receptors. ChemPhysChem 5, 327–335.

Rinnerthaler, M., Bischof, J., Streubel, M.K., Trost, A., Richter, K., 2015. Oxidative stress in aging human skin. Biomolecules 5, 545–589.

Rudmann, D.G., Alston, J.T., Hanson, J.C., Heidel, S., 2013. High molecular weight polyethylene glycol cellular distribution and PEG-associated cytoplasmic vacuolation is molecular weight dependent and does not require conjugation to proteins. Toxicol. Pathol. 41, 970–983.

Sahoo, N.G., Kakran, M., Shaal, L.A., Li, L., Müller, R.H., Pal, M., Tan, L.P., 2011. Preparation and characterization of quercetin nanocrystals. J. Pharm. Sci. 100, 2379–2390.

Schäfer-Korting, M., Mehnert, W., Korting, H.-C., 2007. Lipid nanoparticles for improved topical application of drugs for skin diseases. Adv. Drug Deliv. Rev. 59, 427–443.

Shen, Z., Fisher, A., Liu, W.K., Li, Y., 2018. PEGylated “stealth” nanoparticles and liposomes. In: Parambath, A. (Ed.), Engineering of Biomaterials for Drug Delivery Systems. Woodhead Publishing, pp. 1–26.

Stemmelen, M., Travelet, C., Lapinte, V., Borsali, R., Robin, J.-J., 2013. Synthesis and self-assembly of amphiphilic polymers based on polyoxazoline and vegetable oil derivatives. Polym. Chem. 4, 1445–1458.

Tan, Q., Liu, W., Guo, C., Zhai, G., 2011. Preparation and evaluation of quercetin-loaded lecithin-chitosan nanoparticles for topical delivery. Int. J. Nanomed. 6, 1621–1630.

Valacchi, G., Sticozzi, C., Pecorelli, A., Cervellati, F., Cervellati, C., Maioli, E., 2012. Cutaneous responses to environmental stressors. Ann. N. Y. Acad. Sci. 1271, 75–81.

Verbraeken, B., Monnery, B.D., Lava, K., Hoogenboom, R., 2017. The chemistry of poly(2-oxazoline)s. Eur. Polym. J. 88, 451–469.

Viegas, T.X., Fang, Z., Yoon, K., Weimer, R., Dizman, B., 2018. 6 - Poly(oxazolines). In: Parambath, A. (Ed.), Engineering of Biomaterials for Drug Delivery Systems. Woodhead Publishing, pp. 173–198.

Wang, J., Zhao, X.H., 2016. Degradation kinetics of fisetin and quercetin in solutions affected by medium pH, temperature and co-existing proteins. J. Serb. Chem. Soc. 81, 243–254.

Yang, L., Li, P., Gao, Y.-J., Li, H.-F., Wu, D.-C., Li, R.-X., 2009. Time Resolved UV-Vis Absorption Spectra of Quercetin Reacting with Various Concentrations of Sodium Hydroxide.

Yi, X., Kabanov, A.V., 2013. Brain delivery of proteins via their fatty acid and block copolymer modifications. J. Drug Target. 21, 940–955.

Zalipsky, S., Hansen, C.B., Oaks, J.M., Allen, T.M., 1996. Evaluation of blood clearance rates and biodistribution of poly(2-oxazoline)-grafted liposomes§. J. Pharm. Sci. 85, 133–137.